Neuroscience Vol. 41, No. 2/3, pp. 351–364, 1991
Printed in Great Britain

0306-4522/91 $3.00 + 0.00
Pergamon Press plc

THE THALAMIC CLOCK: EMERGENT NETWORK PROPERTIES

G. BUZSÁKI*

Department of Neurosciences M-024, University of California at San Diego, La Jolla, CA 92093, U.S.A.

Abstract—Rhythmical oscillation of thalamic neuronal populations occurs under physiological conditions and in several disease states. In the present experiments we examined the network properties of population rhythmicity and the possible involvement of *N*-methyl-D-aspartate receptors in the frequency regulation and maintenance of rhythmic thalamic bursts. Multisite recording of neuronal activity and local microinjections of drugs were performed on the freely moving rat. Rhythmic thalamic population bursts at 6 to 9 Hz and concurrent neocortical high voltage spike-and-wave spindles were observed during awake immobility, with the thalamic rhythm leading the neocortical high voltage spindle. Even though all individual thalamocortical neurons fired in a phase-locked manner to the high-voltage spindle, the majority discharged at a significantly lower frequency than that of the population (multiunit) activity. In contrast, neurons in the nucleus reticularis thalami discharged at the frequency of the population bursts. Neurons in the extrapyramidal system and neocortex but not the hippocampal formation also fired in a phase-locked manner to the high-voltage spindle. Systemic administration or local microinjection of either non-competititve or competititve *N*-methyl-D-aspartate blockers (ketamine or ap-5) slowed the frequency of thalamic multiunit bursts and associated high-voltage spindles from 8 to 2 Hz, or completely blocked rhythmicity. Unilateral thalamic injection of ketamine or ap-5 resulted in a suppression of the amplitude of high-voltage spindles in the injected hemisphere.

It is concluded that thalamic rhythmicity is not due to the "pacemaker" properties of thalamic cells but is rather an emergent property of the relay thalamus–nucleus reticularis network. Furthermore, we hypothesize that the frequency of network oscillation is regulated by the interplay between two major classes of voltage-dependent conductances in the thalamocortical cells: low-threshold calcium channels and high-threshold *N*-methyl-D-aspartate channels.

Rhythmic, bilaterally synchronous electroencephalogram (EEG) patterns in the neocortex occur under physiological conditions and during disease states. In humans, the best known examples are sleep spindles at 12–14 Hz, occipital alpha and somatosensory mu rhythms at 6–8 Hz, and spike-and-wave discharges at about 3 Hz in patients with *petit mal* epilespsy. A common origin of these patterns has long been suspected,[22] mainly based on the observation that arousing stimuli tend to suppress all rhythmic patterns in the neocortex.[12,38,45,48] The findings that neocortical rhythmic patterns in animals have different frequency ranges but frequency ratios similar to those in humans have led to the suggestion that these patterns may be brought about by a common rhythm generator or "pacemaker" with the various slow patterns resulting from frequency division(s) at some level between the rhythm generator and the neocortex.[14,15,26,27,32,45]

Although earlier works supported the view that rhythmic patterns are generated in the neocortex,[28] a consensus today is that neocortical rhythmicity is due to the oscillatory behavior of the intrathalamic or thalamocortical circuitry.[1,46] Regarding frequency changes, it was specifically suggested that barbiturate spindles at 8–10 Hz in cats are converted into spike-and-wave patterns of 4–5 Hz after penicillin administration due to diffuse hyperexcitability and consequent enhanced recurrent inhibition of neocortical neurons.[3,15,17,27] Thus, the output of an unchanged thalamic clock was proposed to be divided at the cortical level due to the periodic refractoriness of neocortical neurons brought about by enhanced recurrent inhibition.

If the ultimate source of neocortical rhythmicity is the thalamus, how is the oscillatory pattern organized in this structure? The "facultative pacemaker" model of Andersen and Andersson[1] assumed that any nucleus in the thalamus is capable of sustaining rhythmic patterns through cyclic excitation and recurrent inhibition via local interneurons. Rhythm "distributor" cells with widespread internuclear connections were hypothesized to synchronize the various thalamic nuclei. The major problems with this model are that internuclear or intranuclear recurrent collaterals of the thalamocortical cell are extremely sparse,[23,36,60,61] and GABAergic interneurons are absent in the major thalamic nuclei of the rat.[18]

Two recent discoveries have further advanced our understanding of thalamic oscillation. Firstly, thal-

*Present address: Center of Molecular and Behavioral Neuroscience, Rutgers University, 195 University Avenue, Newark, NJ 07102, U.S.A.

Abbreviations: EEG, electroencephalogram; HVS, high-voltage spindle(s); NMDA, *N*-methyl-D-aspartate; RT, nucleus reticularis thalami; VL, VM and VPM, ventrolateral, ventromedial and ventralis posteromedial nuclei of the thalamus, respectively.

amic neurons were found to possess a low threshold Ca^{2+} spike mechanism which allows them to burst rebound spikes when a hyperpolarized cell is quickly released from inhibition.[11,19,20,47] Secondly, selective damage of the GABAergic nucleus reticularis thalami (RT) was shown to abolish thalamic and neocortical rhythmic patterns in the cat[50] and the rat.[5] These and other findings led Steriade to suggest that the RT is a true "pacemaker", and its neurons impose their rhythmicity onto follower elements in the various thalamic nuclei.[50,52] It remained to be elucidated, however, how rhythmic firing of individual GABAergic RT neurons become entrained into network oscillation.

The present experiments addressed two major issues. Firstly, can the neocortical rhythmic patterns with various frequencies be explained by alteration of the thalamic clock frequency? Secondly, are the thalamocortical neurons actively involved in the network oscillation or do they simply follow the command input of the RT? Fischer 344 rats were used in the present experiment because they display very high-voltage spindles (HVS) with easily detectable spike-and-wave components.[5,6] HVS are present in the awake but immobile rat, thus they are distinct from the 12–16 Hz lower amplitude sleep spindles. Multisite recording of neuronal activity and local microinjections of drugs were used in the freely moving animal.

EXPERIMENTAL PROCEDURES

Surgery

The experiments were carried out in three- to 20-month-old female rats of the Fischer 344 strain ($n = 40$). Rats were anesthetized with a mixture of ketamine (100 mg/kg), xylazine (5.2 mg/kg), and acepromazine (1 mg/kg) and placed into a stereotaxic apparatus. Stainless steel screws (0.5 mm diameter) were used as epidural recording electrodes using the following coordinates, relative to bregma: L = 2.5 mm, AP = 2.5; L = 5.0, AP = 0.0, bilaterally. These coordinates were chosen because previous mapping experiments showed that HVS has their amplitude maxima at these locations.[6] In addition to the epidural EEG recording screws, three types of depth recording electrodes were used: single wire microelectrodes, multielectrodes, and chemotrodes. In experiments with a single microelectrode a microdrive socket (5.0 mm i.d.) was secured above a 4-mm hole in the skull with dental acrylic. For recording from neurons in RT and n. ventralis lateralis (VL) of the thalamus the center of the hole was at AP = −1.8 mm and L = 2.5 mm. In animals with multielectrodes an array of 16 tungsten wires (50 μm) with 250 μm horizontal separation was used to record simultaneously from adjacent nuclei of the thalamus (AP = −1 to −3.6, L = 2.0, V = −5.0 to −7.0) or from the caudate nucleus, pallidum and thalamus. The electrode assembly was moved by means of three screws whose filed heads were embedded in dental acrylic.[7] In all rats, two screw electrodes driven into the bone above the cerebellum served as indifferent and ground electrodes.

The chemotrode consisted of a guide cannula (26-gauge) with a pair of 60-μm wires glued to it. The wires were cut so that the tips were 1.0 mm apart, with the longer wire protruding 0.5 mm beyond the tip of the cannula. Two such chemotrodes were implanted symmetrically into the sensorimotor cortex (AP = 1.0, L = 2.5, V = −1.0) with the deep electrode aiming layer V. Simple cannulas (26-gauge) for drug delivery were implanted in the thalamus (AP = −1.8, L = 2.0, V = −6.0). The guide cannula accepted a 33-gauge inner cannula through which drugs in 0.5 μl volume were delivered. Drugs [*N*-methyl-D-aspartate (NMDA), Sigma; ap-5, Tocris Neuramin; ketamine–HCl, Aveco] were freshly dissolved in phosphate-buffered saline and delivered (at a speed of 0.2 μl/min) by a 1 μl Hamilton syringe connected to the inner cannula with flexible tubing. During the drug delivery the rat was gently restrained. Control injection consisted of 0.5 μl volume of saline. When drugs were infused unilaterally, the contralateral hemisphere was injected with saline. At least 36 h elapsed between successive drug or vehicle injections.

Recording, stimulation and data processing

A multichannel Mosfet input operational amplifier system, embedded into the female connector, was used to eliminate cable movement artifacts.[7] During the recording sessions the rat was left in its home cage and placed on a recording platform. A sensitive magnet-coil velocity detector inside the platform allowed monitoring of the movement of the rat and the precise timing of movement relative to bioelectric events. EEG activity was recorded on an eight-channel polygraph and stored on magnetic disc (AST-AT) after digitalization of the traces at 200 Hz. The EEG was band-pass-filtered at 1–75 Hz. An additional active (40 dB/octave) band-pass filter (5–75 Hz) was used to enhance the detection of neocortical HVS. Raw EEG and its filtered derivative was displayed on the computer screen to facilitate visual detection of rhythmic patterns.

A recording session lasted until 30 min of EEG data, recorded during cumulative awake immobility epochs, was collected. If movement occurred within 20 s of an EEG epoch, the data were discarded. Thus, the EEG activity reported in this paper reflects neocortical activity of relatively stationary awake immobility with head up and eyes open. If the rat assumed a sleeping posture and/or slow delta waves began to appear in the EEG the rat was aroused by touching its vibrissae gently or by lifting it up.

Three different methods were used to quantitatively evaluate HVS. Firstly, the spike components were detected on-line by an amplitude-discriminator program on-line, using a modified version of the R.C. Electronics software package (Santa Barbara, CA). The threshold value was preset at a level twice the amplitude of the background EEG. The digital output pulses of the discriminator (Fig. 1) were fed into a glitch filter set to a value greater than the time interval between the end point of one discriminated spike and the start point of the next spike. The duration of the output pulse of the glitch filter was therefore equal to the duration of the individual HVS episode. The total duration of HVS per session was calculated by multiplying the average duration of HVS by the number of its occurrence. Secondly, the peak amplitudes of the signal occurring within the time window of the window-discriminator onset and offset were determined and the values used to construct amplitude histograms. Thirdly, Fourier analysis was carried out on the raw EEG using a Fast Fourier Transform program. The derived power spectra were displayed between 0.5 and 25.5 Hz. The power values were arbitrary but the scale remained identical within the same animal and across drug manipulations. Statistical comparisons were made by paired *t*-tests. Up to 16 channels of EEG and/or unit data could be processed this way.

Unit activity (500 Hz–8 kHz) was discriminated by window discriminators or by a pattern recognition software program (R.C. Electronics). In the case of multiple unit recordings, a glitch filter software was used with a 10 or 20 pulse width to exclude accumulation of bits at short intervals. For peri-event histograms, interspike interval histograms, and amplitude histograms, the mean, mode, median, and standard deviation were calculated.

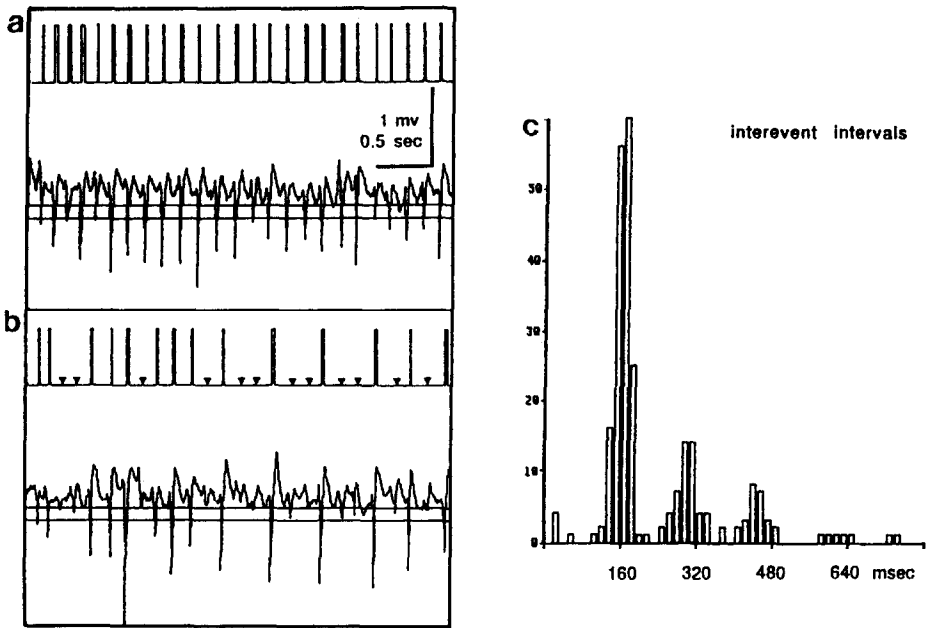

Fig. 1. HVS with regular (a) and irregular (b) spike components recorded from the frontal cortex in a F344 rat. The two traces were recorded within a 1-min interval. Trace b is atypical. The uniform pulses above the EEG traces indicate the occurrence of spike components. The threshold level is indicated by the lower horizontal line. Upper horizontal line: reset of the threshold discriminator. Arrowheads in b indicate the absence of spike components and/or failures of detection. Spike failures occurred with equal probability after large and small amplitude spike components. Note the regular frequency of the spike components (a) and their re-occurrence at about the same "clock" frequency even after failures (b). (c) Histogram of the interspike intervals of HVS. Note the dominant frequency at 160-ms intervals and smaller peaks at about 300 and 400 ms. The histogram is based on 0.5 h of EEG data recorded during awake immobility. Positivity is up in this and all subsequent figures.

Histological methods

The animals were deeply anesthetized and perfused via an intra-aortic cannula with 0.1 M phosphate-buffered saline (50 ml) followed by ice-cold 4.0% paraformaldehyde. The brains were removed, equilibrated in 30% sucrose for two days, and then sectioned in the coronal plane at 40 μm on a freezing microtome. Sections were stained for Nissl substance with thionin. In the vicinity of the electrode tracks and cannula every section was stained. Recording sites at different depths were reconstructed from the final position of the tip of the electrodes on the histological sections and for calculations of the number of turns of the microelectrode drive.

RESULTS

HVS occurred almost exclusively during immobility. An ongoing HVS episode could be interrupted by picking the animal up or forcing it to move, or by loud acoustic stimuli. The intraspindle frequency was usually highest (8–11 Hz) after onset and then slowed down to 6–7 Hz for the duration of the HVS. In agreement with previous findings,[2,6,56] the incidence (range: 1–50/h) and duration (range: 0.8–60 s) of HVS episodes increased with age. HVS were easy to recognize even at very low chart paper speeds as their amplitudes were three to five times greater than the background desynchronized EEG. In some animals the spike components of the epidurally recorded HVS reached 5 mV. The average duration of HVS decreased during drowsy states in which large amplitude, irregular delta waves were present and during sleep. These behavioral states were often accompanied by short duration (0.2–2 s) high-frequency (12–14 Hz) spindles. Sleep spindles were easily seen on the oscilloscope as bursts of rhythmic sinusoid waves; their amplitudes did not substantially exceed the amplitude of the background EEG and they lacked spike components.

Closer examination of the HVS revealed that spike components sometimes failed to occur (Fig. 1). Following a failure the next spike component reappeared after a delay which was approximately twice or three times longer than the average interspike interval of the HVS. This relationship is quantitatively reflected by the presence of several peaks in the interspike interval histograms at regular intervals (Fig. 1c). These findings suggest that timing of the spike-and-wave activity is not regulated by neocortical neural groups in the vicinity of the recording electrode, but by a clock input located elsewhere. If HVS emerged from the local neocortical circuit one would expect to see longer interspike intervals following large spike components than after small ones. Our observations suggest the contrary.

Simultaneous recording of neocortical and thalamic EEG and thalamic unit activity is shown in Fig. 2. Inspection of the EEG traces alone would lead to the conclusion that rhythmicity begins in the neocortex and is followed by the thalamus. However,

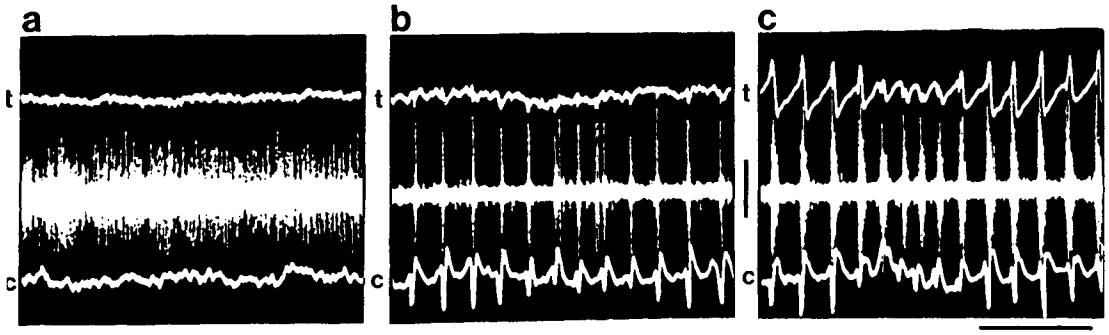

Fig. 2. Relationship between thalamic EEG (t, upper trace), thalamic multiple unit activity (middle trace) and neocortical EEG (c, lower trace). Panels a–c illustrate samples before the onset of HVS (a), during the initial part of HVS (b) and later part of HVS (c). Note that local EEG patterns in the thalamus (t traces) do not always reflect rhythmic population bursts of thalamocortical cells (e.g. in panel b), but when further cells are recruited, population rhythmicity is also obvious in the local micro-EEG (trace t in panel c). Calibrations = 0.5 s; 0.5 mV (t), 1 mV (c), 0.2 mV (unit trace).

simultaneous recording of multiple unit activity clearly revealed that rhythmic population bursts were present in the thalamus, several hundred milliseconds before EEG rhythmicity, recorded from the tip of the microelectrode, became obvious. It was not until a substantial number of thalamic neurons were recruited into population bursts that the field EEG reflected thalamic rhythmicity (Fig. 2c). Numerous episodes of HVS in 13 rats showed this relationship consistently. HVS were never observed without clear-cut rhythmic discharges of neurons in the VL. On the other hand, large amplitude field EEG rhythmicity in the thalamus very frequently preceded neocortical HVSs, confirming previous observations.[57]

Population synchrony in the thalamus during high-voltage spindle

Simultaneous multisite recording of unit activity of thalamic neurons during HVS is shown in Fig. 3. As a rule, thalamocortical neurons discharged predominantly during the spike components of the epidurally recorded HVS. Visual analysis of hundreds of records indicated that there was not a simple relationship between the amplitude of the spike components of HVS and the synchrony of multiple unit discharges at a given electrode location. Population bursts were usually initiated by neurons at one or two recording sites with neurons at other sites recruited into the population events one to three cycles later (Fig. 3a).

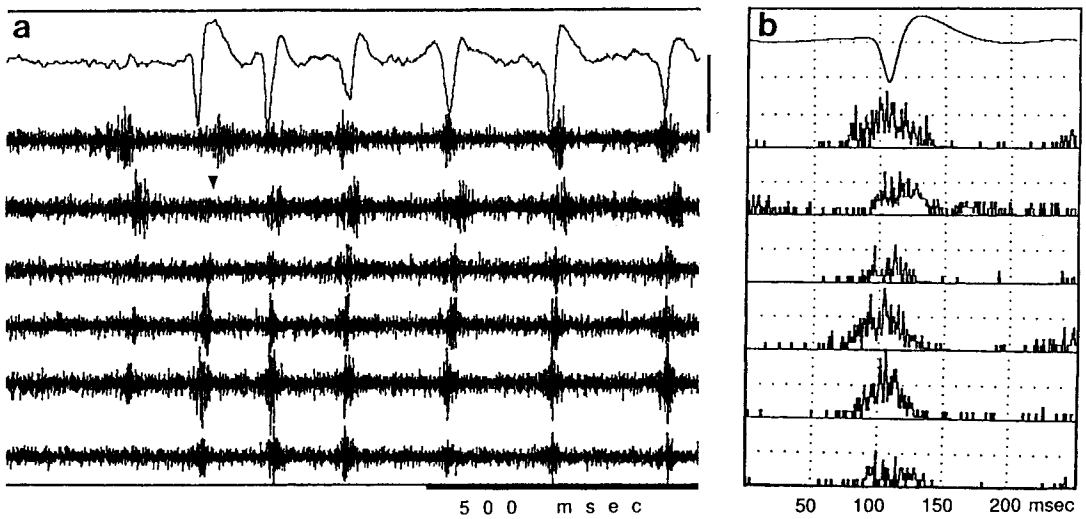

Fig. 3. Recruitment of the thalamic neuronal network during HVS. (a) Simultaneously recorded subpopulations of neurons in the ventrolateral nucleus (unit traces 1–4) and posterior nucleus (traces 5, 6) of the thalamus. The recording electrodes were spaced at 250-μm intervals in the sagittal axis. Uppermost trace: epidural recording from above the sensorimotor cortex. Note the initial jitter and subsequent phase-locking of unit firing with the spike components of HVS. Population bursting may have been initiated by neurons of the first unit trace. Arrowhead indicates an omission of population burst. Note also that rhythmic thalamic population bursts preceded the neocortical EEG change. (b) Peri-event histograms of multiple unit activity triggered by the peak of the spike component of HVS. Histograms are averages of 50 repetitions. Calibrations = 1 mV (EEG), 400 μV (unit).

Initially, there was a considerable jitter between population bursts at different locations; this jitter decreased substantially after the onset of the neocortically recorded HVS. Sometimes, omissions of population bursts were observed at one or several locations (in conjunction with the HVS), but subsequent neuronal bursts emerged at the time of the overall population synchrony (Fig. 3). These findings suggested that collective behavior of large neuronal aggregates is a better predictor of neocortical patterns than multiple unit activity recorded only at any one site. Therefore, in subsequent experiments we examined the discharge properties of isolated thalamocortical neurons during HVS and compared their behavior to population rhythmicity.

A total of 108 individual cells in the VL, ventromedial and ventralis posteromedial nuclei of the thalamus (VM, VPM, respectively) and posterior thalamic nucleus in seven rats were held long enough to construct interspike interval histograms and cross-correlograms with the neocortically recorded HVS. Cross-correlation with HVS, similarly to multiple unit activity, revealed that all isolated thalamocortical neurons discharged preferentially during the spike component of HVS. In agreement with previous *in vivo* observations,[5] thalamocortical cells often displayed bursts of several spikes of decreasing amplitude during HVS (Fig. 4a), while mainly single spikes were observed during movements and during immobility periods without HVS. Unlike multiple unit activity, individual thalamic neurons very rarely fired rhythmically. Most cells decreased their overall firing rates at the onset of neocortically recorded HVS. Rhythmic discharges for two to five consecutive cycles of HVS were observed occasionally, with the cell remaining silent for long periods or firing action potentials at intervals several-fold longer than the frequency of HVS. An interspike interval histogram of a typical thalamocortical neuron is illustrated in Fig. 4c. The small peak at HVS frequency is in contrast to the large peaks of interspike interval histograms derived from multiple unit activity (Fig. 4b, d). These findings suggest that rhythmic population synchrony in the thalamus is a collective property of neurons, a feature not predictable from observations of single cell behavior.

As discussed above, population synchrony of thalamocortical cells often preceded the onset of neocortical HVS. We attempted to quantify this observation by peri-event averaging of neuronal discharges. Using off-line analysis, we selected the very first spike components of successively occurring HVS episodes to trigger the averager. Neuronal activity from 17 locations in the VL in six rats was analysed this way. In all but two of the 17 averages, rhythmic

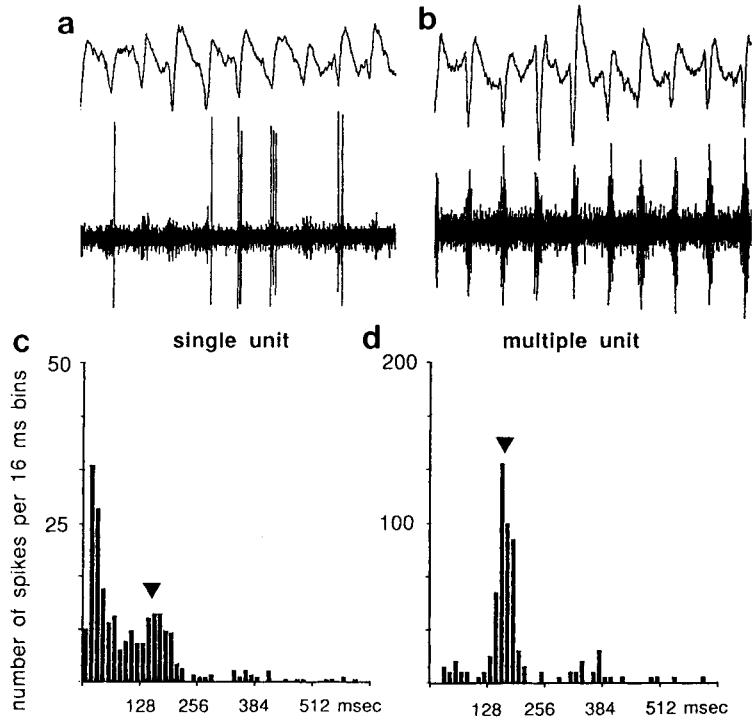

Fig. 4. Relationship between individual and population behavior of thalamic neurons (VL nucleus) during HVS. (a) Neocortical EEG and action potentials of a typical single VL neuron. Note phase-locking of cell-firing to the spike component of HVS and its low level of rhythmicity. (b) Neocortical HVS and multiple unit activity in VL. Note phase-locking and high level of rhythmicity. (c) and (d) Interspike interval histograms of units shown in (a) and (b), respectively. Triangles indicate modal intervals of the spike components of HVS recorded simultaneously (not shown). Note the small histogram for the single cell (c) and the large peak for multiple unit activity (d) at HVS frequency.

peaks of thalamic unit activity were obvious before the occurrence of HVS in the neocortex (Fig. 5).

High-voltage spindle and neuronal rhythmicity in various structures

Although this study was not designed to systematically map the various anatomical structures that show HVS-concurrent rhythmic modulation of neurons, we have collected quantitative information from large numbers of neurons of the neocortex, hippocampal formation, thalamus and the extrapyramidal system. A neuron of neuronal population was considered to be affected by HVS if the cross-correlogram revealed a peak at least twice as large as the randomly shuffled average. In agreement with previous reports[3,5,27,54] all neurons in the somatosensory and parietal neocortex, including isolated putative interneurons, fired in conjunction with the spike component of HVS ($n > 100$). In contrast, none of the more than 200 units/multiple units examined in the CA1–CA3 fields of the hippocampus, dentate gyrus and subiculum of the dorsal hippocampal formation showed any reliable modulation of cellular firing during HVS. Reliable rhythmic modulation of HVS frequency was present at 189 of the 195 thalamic recording sites examined, including the VL, VM, VPM, n. ventralis posterolateralis, RT, laterodorsal nucleus and posterior nucleus. All thalamocortical cells fired during the spike component of HVS. In contrast, the majority of RT units discharged during the wave component of HVS. No HVS-related rhythmicity was present in two units in the lateral habenula in two rats. Of the nine multiunit recordings in the caudate nucleus six cross-correlograms showed small but significant peaks. HVS-associated modulation of the neurons was also evident in four multiple units of the pallidum and two single units in the zona incerta. These findings suggest that many areas of the brain are affected by the HVS-associated rhythmicity; however, limbic structures are not involved.

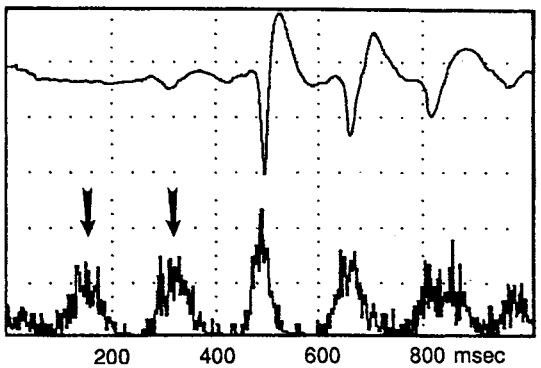

Fig. 5. Relationship between neocortical EEG and thalamic rhythmicity (VL nucleus). Peri-event averages of neocortical HVS episodes and thalamic unit firing triggered by the peak of the spike component of HVS. For these averages HVS with large first spike components were selected off-line and averaging was initiated only by the very first spike component of successive HVS episodes ($n = 50$). Note rhythmic peaks of multiple unit activity in the thalamus (arrows) before the onset of the HVS. Vertical scale = 0.25 mV.

High-voltage spindle and N-*methyl*-D-*aspartate receptors*

Drugs affecting the catecholamine systems have been reported to affect the incidence and duration of HVS episodes without significantly altering the intraburst frequency of HVS.[24,33] In addition, we found that intraperitoneal injection of the non-competitive NMDA antagonist ketamine substantially decreased the frequency of HVS both with and without pretreatment of the animal with the alpha-2 adrenoceptor agonist xylazine (1 mg/kg) or the major tranquillizer acepromazine maleate (1 mg/kg).[8] The effect of low doses (< 50 mg/kg) of ketamine was difficult to evaluate because the animals displayed almost continuous ataxia (HVS were never observed during movement). A dose of 100 mg/kg rendered the rat motionless within 5 min. The frequency of HVS showed a continuous decrease with post-injection time and could be as slow as 1.6 Hz (Fig. 6a–c). The effect was always transient and after 15–25 min rhythmicity was no longer present. HVS reappeared in parallel with the recovery from anesthesia but its frequency was always lower than that recorded without ketamine treatment (Fig. 6d).

In order to reveal the neuronal targets of ketamine, involved in the frequency regulation of HVS, we injected small volumes of the drug directly into the thalamus ($n = 7$) or the sensorimotor cortex ($n = 4$). Bilateral injection of ketamine (100 nmol in 0.5 μl volume) into the VL/RT significantly decreased the frequency of HVS ($P < 0.02$; paired t-test), similar to peripheral administration. In contrast, injection of very high doses of ketamine (500 or 1000 nmol) into the neocortex did not change the frequency of HVS either locally or distally ($n = 4$).

To further evaluate the involvement of NMDA mechanisms in thalamic oscillation, we tested the effects of unilateral ($n = 16$) and bilateral thalamic injections ($n = 5$) of the specific NMDA antagonist ap-5 as well as the effects of NMDA itself. Bilateral injections of small quantities of ap-5 (1–10 nmol/0.5 μl) also significantly decreased the frequency of neocortical HVS (Fig. 6e–h) ($P < 0.05$ at 1 nmol; $P < 0.02$ at 10 nmol). Soon after the injection the pre-drug HVS of 6–8 Hz were interspersed with HVS of 3–4 Hz. Eventually the frequency of HVS could be as low as 2 Hz. Occasionally, spike-and-wave patterns of 6–8 Hz were superimposed on the very slow HVS (Fig. 6e). After about 1 h the frequency of HVS returned to pre-drug levels. Following bilateral injection of NMDA (25 nmol), animals ($n = 3$) displayed continuous movements for up to 1 h; HVS were absent. Bilateral injections of saline alone ($n = 5$) produced no change in the frequency of HVS.

Unilateral injection of ap-5 into the thalamus ($n = 9$) resulted in frequent ipsilateral circling interspersed with immobility periods. During immobility,

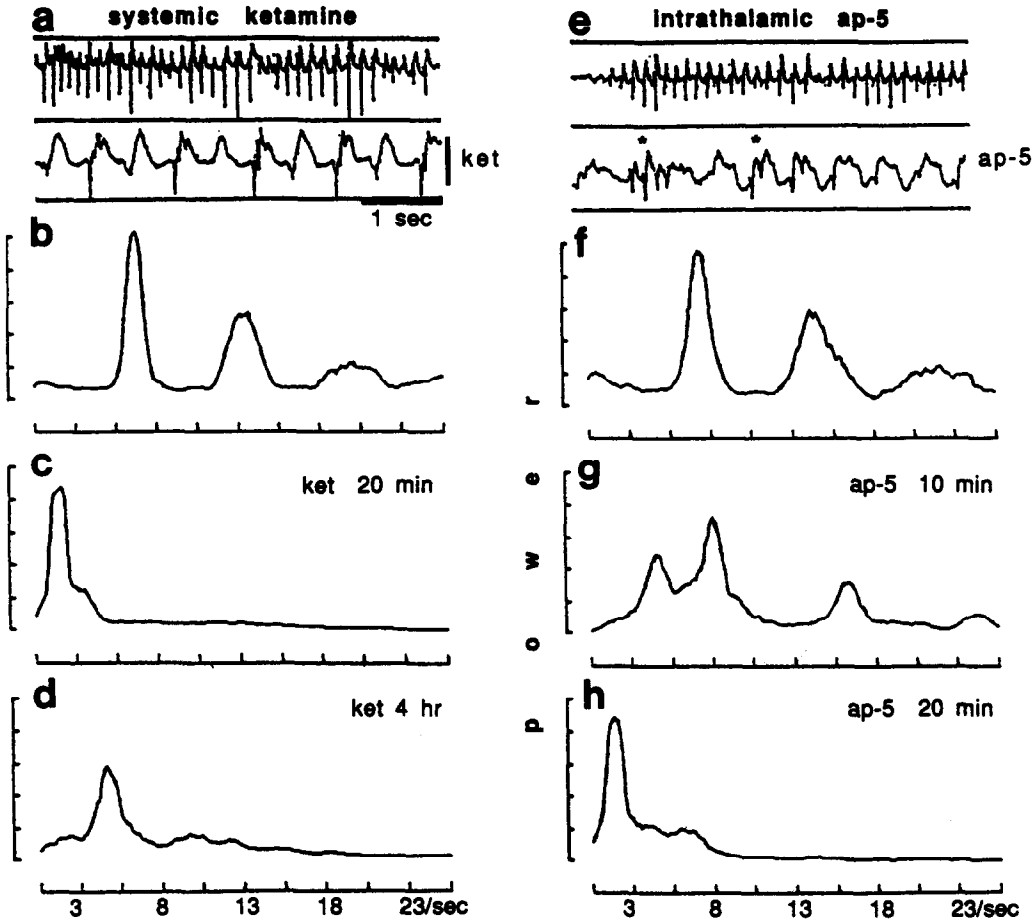

Fig. 6. Effect of bilateral injection of ap-5 into the ventrobasal thalamus of EVS. (a) EEG samples of HVS recorded from above the sensorimotor cortex before (upper trace) and after intraperitoneal administration of ketamine (ket trace; 50 mg/kg). Note slow (about 2 Hz) spike-and-wave pattern after ketamine. The rat was pretreated with xylazine to increase the incidence of HVS. (b–d) Power spectra obtained before (b), and 20 min (c) and 4 h (d) after ketamine administration. Between 25 min and 4 h post-ketamine no rhythmic patterns were present. Peak at 4–5 Hz at 4 h reflects the emergence of HVS with the recovery from anesthesia. (e) Neocortical EEG samples of HVS before (upper trace) and after (ap-5 trace) bilateral microinjection (0.5 μl) of 1 nmol ap-5 into the VL. Note slow (2 Hz) rhythmicity after ap-5. Asterisks indicate mixtures of HVS at 7 and 2 Hz. (f–h) Power spectra of EEG before (f) and 10 min (g) and 20 min (h) after ap-5 microinjection. Note the emergence of a power peak at about 3–4 Hz after 10 min (g) and the dominance of 2 Hz rhythmicity later (h). Ordinates: arbitrary units. Bilateral saline injections in control sessions produced no changes in HVS frequency (not shown).

rats assumed a curved posture leaning towards the injected side. HVS, when present, were usually of the same frequency on both sides (6–8 Hz), but the amplitude of the HVS was significantly lower on the side injected with ap-5 than on the vehicle-injected side. Averages of HVS (Fig. 3b) were obtained for all four recording locations by using the spike component of the HVS derived from the sensorimotor area of the vehicle-injected hemisphere as a trigger. Comparisons of the interhemispheric amplitude ratios of the average waveforms indicated that the amplitude of the HVS decreased 38% after 1 nmol ($P < 0.01$) and 65% after 10 nmol ap-5 injections ($P < 0.002$). This amplitude decrease was further evaluated by comparing power peaks at 6–8 Hz and measuring the amplitude of the individual spike components of HVS (Fig. 7). Power peak comparisons of the EEG of the drug- and vehicle-injected hemispheres allowed us to determine the minimum effective dose of ap-5 (Table 1). Even though the results obtained with the lowest dose (100 pmol/0.5 μl) failed to reach statistical significance at the group level, comparisons of the power spectra within individual rats revealed that even this low dose effectively reduced the amplitude of HVS in four of the 10 hemispheres tested ($P < 0.05$; t-test). These four hemipheres also showed the largest power decrease with the higher doses of ap-5. In two rats, the power peak at about 2 Hz significantly increased on the drug-injected side (Fig. 7).

Unilateral injection of 25 nmol/0.5 μl NMDA ($n = 4$) induced very rapid contralateral circling and

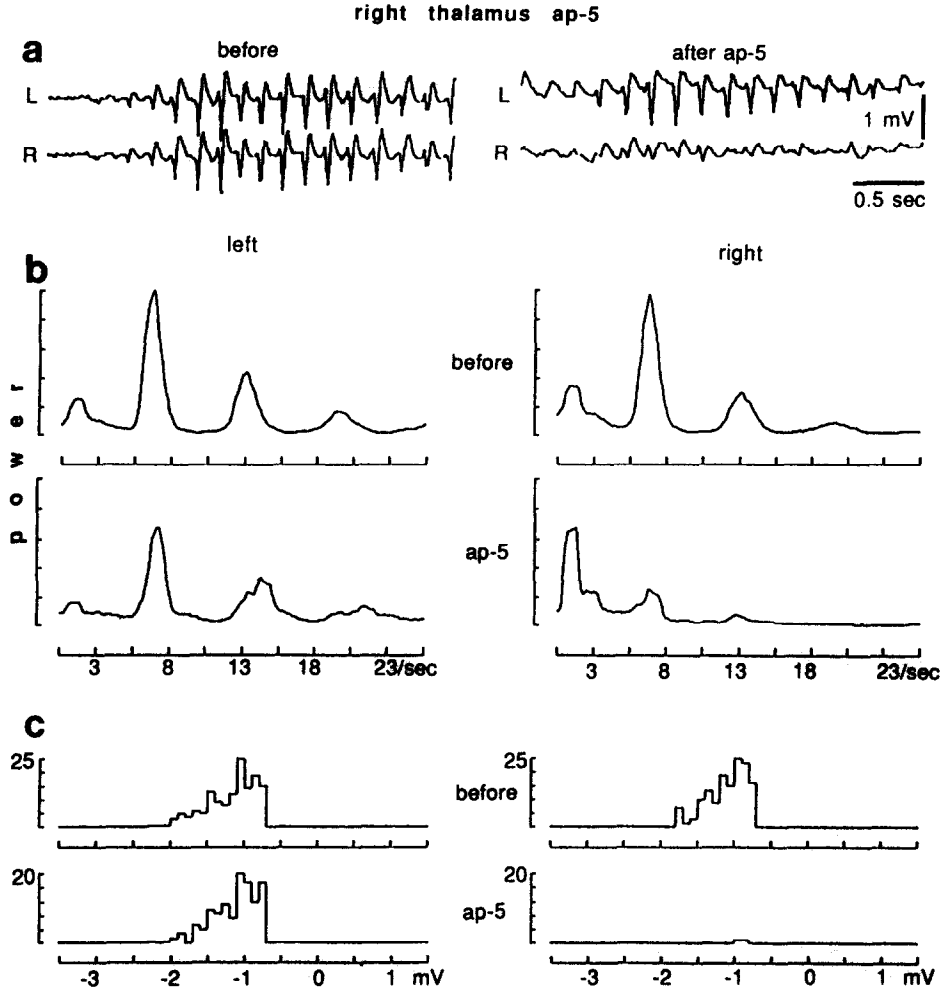

Fig. 7. Effect of unilateral blockage of NMDA transmission in the thalamus of HVS. (a) HVS recorded from the left (L) and right (R) sensorimotor cortex before and after ap-5 (10 nmol) microinjection into the right VL. Note amplitude decrease of HVS on the injection side (right, lower trace). The left thalamus was injected with saline (0.5 μl) only. (b) Power spectra of EEG before and after the ap-5 injection. Note substantial decrease of the power peaks at 6–7 and 13 Hz and increase of the 2 Hz peak of the ap-5-injected side. (c) Amplitude histograms of the spike components of HVS. Note the absence of large amplitude spike components on the ap-5 injection side (right, bottom).

occasional rotations along the longitudinal body axis away from the injected side. Circling behavior was quantified in one rat. This animal displayed 118 contralateral and five ipsilateral turns in 30 min. Twitching of the contralateral vibrissae and forelimb and slow rearing were also observed occasionally. These behaviors were strikingly similar to behavior patterns observed in the course of kindling-induced seizures[39] with the exception that the neocortex displayed a desynchronized EEG at all times. Because of frequent circling and rare immobility periods, HVS were observed in only two rats. In these animals the frequency of HVS was comparable to pre-drug values. However, the amplitude of the spike component increased 20 and 22%, relative to the vehicle-injected side. Another important difference was that HVS also occurred during small head movements; in untreated rats HVS were present only during complete immobility. The animals assumed a curved body posture away from the NMDA-injected hemisphere during brief immobility periods.

Table 1. Effect of intrathalamic ap-5 on high-voltage spindle

Dose	n	Percentage decrease*	$P <$
10 nmol	9	58	0.001
1 nmol	19	49	0.002
500 pmol	10	36	0.05
100 pmol	10	24	0.055

*Percentage decrease of HVS power relative to vehicle-injected side.

The last series of experiments examined the effect of systemic ketamine administration on the rhythmicity of thalamocortical neurons. In three rats implanted with single microelectrodes, the effect of

ketamine was successfully investigated on five single units in VL, two of which were from two rats on different occasions. Firstly, cross-correlation histograms—obtained by using the spike component of HVS as a trigger—and interspike interval histograms were constructed. Next, the rat was gently restrained, the injection needle introduced into the peritoneal cavity and if the neuron was not lost, the injection was made. Cross-correlograms revealed that the discharge frequency of the isolated neurons decreased with the HVS (four units). The remaining neuron virtually ceased firing after ketamine administration, precluding post-drug analysis. The effect of ketamine on multiple unit activity in the thalamus was investigated in four rats. As illustrated in Fig. 8, the frequency of rhythmic population bursts in the thalamus decreased at all recording locations following ketamine injection. The intervals between the peaks of the unit cross-correlograms (Fig. 8d) were determined at 15 locations before and after ketamine injections. Peak intervals of 178 ± 21 ms in the undrugged rat increased to 303 ± 65 ms after ketamine administration ($P < 0.001$). In addition, fewer units contributed to the population burst and the peaks of the cross-correlograms were usually wider. At another four recording locations rhythmic neuronal activity was apparent in the drug-free rat but no rhythmicity was detected after drug injection (e.g. electrode 2 in Fig. 8).

DISCUSSION

The major findings of these experiments are that (i) thalamic oscillation is an emergent network property of GABAergic RT neurons and glutaminergic thalamocortical cells, (ii) opening of voltage-dependent NMDA channels may contribute to the rhythmic thalamic bursts underlying neocortical HVS, and (iii) the thalamic clock is the primary determinant of the frequency of neocortical rhythmic events.

Pacemaker neurons or network oscillation

Before presenting our hypothesis about the possible mechanisms of population rhythmicity in the thalamic network, it is appropriate to review the

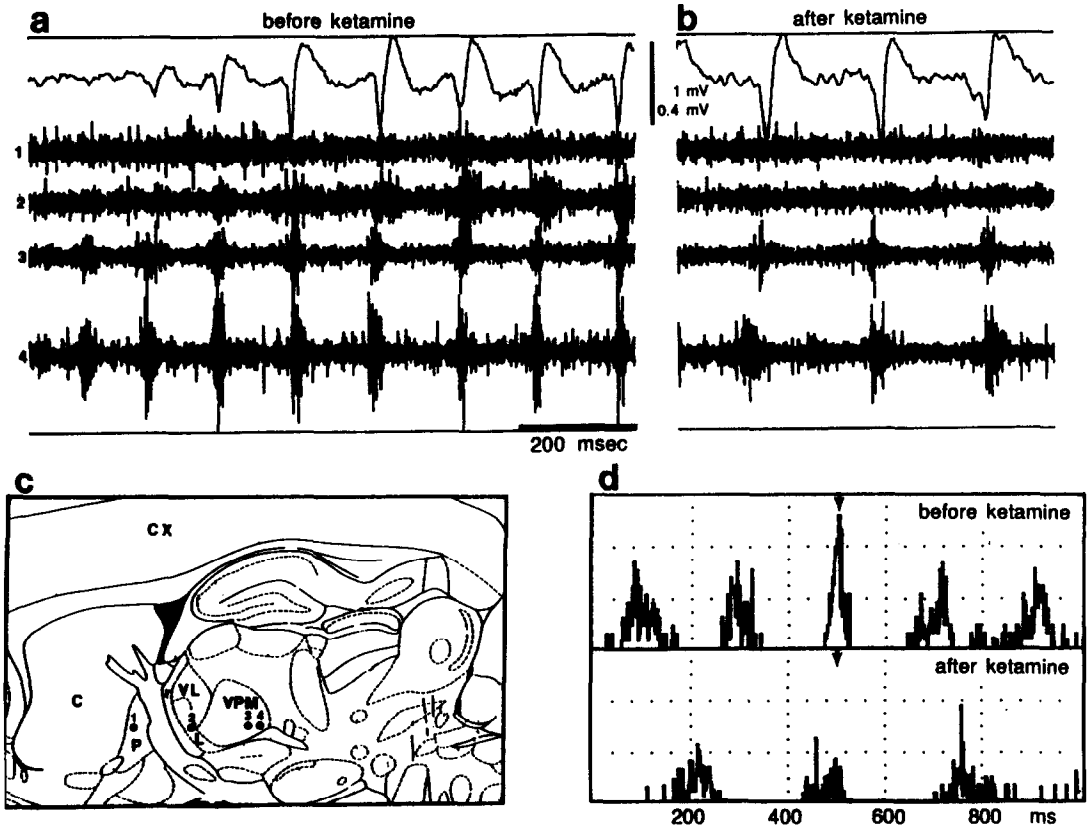

Fig. 8. Frequency shift of thalamic neuronal rhythmicity. (a, b) Neocortical EEG and simultaneously recorded multiple unit activity from the ventral pallidum (trace 1) and thalamus (traces 2–4) before (a) and following ketamine–HCl administration (b) (50 mg/kg, intraperitoneally). Note population rhythmicity in the thalamus and less expressed modulation of pallidal neurons. (c) Schematic illustration of the position of the recording electrodes in the sagittal plane. C, caudate–putamen; CX, neocortex; P, ventral pallidum; L, ventropostero-lateral nucleus; r, reticular nucleus. (d) Peri-event histograms of thalamic unit firing (electrode 4) before and after ketamine administration. Spike components of HVS were used to trigger the peri-event sweeps (arrowheads). Histograms are averages of 50 repetitions. Calibration = 1 mV (EEG), 400 μV (units).

findings that led to the "pacemaker" model of spindle generation. Firstly, axon-sparing lesions of the RT abolish neocortical rhythmicity in both the cat[50] and the rat.[5] More importantly, when the rostral part of the thalamus, including the RT, was isolated from the major part of the thalamus and its neocortical inputs by knife cuts, this island of neurons continued to produce spindles whereas spindles were no longer present in the rest of the thalamus.[52] Secondly, the neurons of the anterior thalamic nuclei and habenula, devoid of an input from the RT,[49,55] do not fire rhythmically during sleep spindles or HVS.[5,35,37] Thirdly, thalamocortical neurons are mainly hyperpolarized during a spindle episode, whereas GABAergic RT neurons[18] discharge virtually continuously during natural sleep spindles in the cat.[51] Furthermore, thalamic neurons discharge almost exclusively during the spike component of HVS,[3,5] whereas most RT cells fire in conjunction with the wave component of HVS. In addition, some RT neurons fire rhythmically at HVS frequency well before the appearance of neocortical HVS.[5] Finally, thalamic neurons possess low-threshold Ca^{2+} channels that allow them to fire with a burst when released from hyperpolarization.[19,20]

The above findings are compatible with the pacemaker hypothesis of the thalamic oscillation.[5,52] According to this model, rhythmic population discharges of GABAergic RT cells phasically hyperpolarize their thalamocortical target neurons so that in the absence of other depolarizing inputs, voltage- and time-dependent rebound spikes occur in a phase-locked manner in these cells. The two major assumptions of this model are: (i) RT cells are genuine pacemaker neurons or neuronal pools that also oscillate in isolation, and (ii) thalamocortical cells merely follow the command input from the RT neurons; their participation is not a prerequisite for rhythmicity in either RT or thalamocortical cells.[5,47,52]

A major issue that has remained to be elucidated in the pacemaker model is how the individual RT neurons become synchronized to provide a phase-locked output. Since recent reports suggest that RT neurons also possess low-threshold Ca^{2+} spikes,[30,31,44] Steriade *et al.*[52] proposed that collective synchrony within the exclusively GABAergic population in the RT is brought about by mutual hyperpolarization–rebound spike sequences. However, some previous observations together with the findings of the present experiments argue against this explanation. Firstly, RT neurons appear depolarized, rather than hyperpolarized, during barbiturate spindles in the cat[46] and the rat.[43] Secondly, during HVS RT neurons *in vivo* fire repetitive spikes of similar amplitude and not bursts of decreasing amplitude, in contrast to the characteristic *decrescendo* discharge patterns of thalamocortical cells.[5] Most importantly the present observation, that blockade of the NMDA channels in thalamic cells can abolish rhythmicity, suggests that glutamate-containing neurons are crucially involved in network oscillation.

A hypothesis is advanced below that encompasses features of the pacemaker model yet accounts for observations not compatible with the pacemaker hypothesis (Fig. 9). In essence, we suggest that thalamic rhythms are brought about by the collective, mutual cooperation of thalamocortical and RT neurons. The sequences of events are envisaged as follows. In the absence of specific and other depolarizing subcortical inputs (e.g. during immobility) thalamocortical cells remain silent (Fig. 2) and only a small portion of these neurons may discharge with bursts. If bursting of some spatially segregated thalamocortical cells (initiator neurons) occurs within a relatively restricted time window (e.g. in Fig. 3) their converging input to RT cells depolarize and discharge RT cells. In turn, the high frequency and synchronous output of these RT neurons will hyperpolarize a number of their thalamocortical target neurons (few-to-many divergence). The hyperpolarizing events may then induce rebound bursting[19,20,40] in some of the affected neurons. These neurons may or may not include initiator cells as the latter may still be refractory due to the burst-induced afterhyperpolarization. These initial events have a dual consequence on the RT–relay thalamus network. Firstly, RT-induced hyperpolarizing effects will be spatially distributed in the thalamocortical cells and secondly, the synchrony of rebound burst discharges of thalamocortical neurons will substantially increase. These events, in turn,

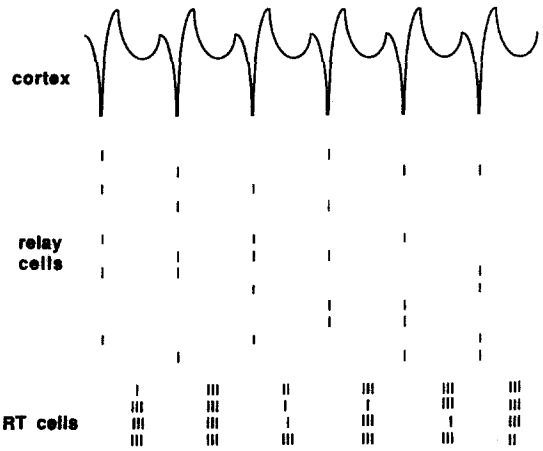

Fig. 9. Diagram of the hypothesized network-generated rhythmicity in the thalamus. Uppermost trace: epidurally recorded HVS (cortex). Vertical bars: action potentials of 14 relay neurons and 5 RT cells. Neither the relay cells nor RT neurons are endowed with intrinsic rhythmicity. Relay cells are not rhythmic but when they discharge their action potentials are phase-locked to the population rhythmicity. RT cells are firing rhythmically at HVS frequency not because they possess pacemaker properties but because of the similar timing of excitation by a converging and relatively constant population of thalamocortical relay cells. Discharge of relay neurons is brought about by RT-induced hyperpolarizations[5,52] and consequent rebound, low-threshold calcium spike activation.[20,21,30]

will recruit more RT neurons to fire in the same phase, and secondarily a larger population of thalamocortical cells will be affected in a time-locked manner during subsequent cycles. Intuitively, this recruitment continues until a large number of RT and thalamocortical neurons are involved in the cyclic oscillation or until recruitment is curtailed by external events.

In this hypothesized network model, RT neurons discharge rhythmically at HVS frequency not because they are endowed with intrinsic pacemaker properties but because of the similar timing of the events in the thalamocortical cell population. Rhythmic firing of individual thalamocortical cells is not necessary and indeed these cells may be silent for long periods or discharge at a much lower frequency than that of HVS (Fig. 4). What is required is an ever varying but relatively constant portion of the thalamocortical cell population that fire rebound spikes in a time-locked fashion. During each cycle a small but relatively constant portion of thalamacortical cells discharge providing a rhythmic thalamofugal output. On the other hand, RT neurons fire rhythmically because of their low threshold and because of the overlapping convergence of thalamocortical cells (many-to-few). Rhythmical firing of RT cells is therefore an emerging property of the network interactions between thalamocortical and RT cells. Low-threshold rebound spikes, mutual connectivity between GABAergic RT cells and thalamocortical neurons and the network rules outlined above are the necessary and sufficient requirements of rhythmic population synchrony in the thalamus. Genuine pacemaker property of individual cells or intrinsically generated intranuclear oscillation (e.g. within RT) is not necessary for the network model in the rat.

It is not intuitively clear, however, why and how the burst-initiator cells discharge in the first place. Possible mechanisms include disfacilitation from subcortical inputs during immobility[5,31,48,52] or transient hyperpolarization of the relay cells by GABAergic afferents from the substantia nigra and the pallidum.[8] Alternatively, a population burst in neocortical cells may activate RT cells which, in turn, may induce rebound spikes in a fraction of the thalamocortical cells. This latter possibility is supported by the empirical observation that single volleys delivered to the sensorimotor cortex effectively induced HVS during immobility.[5]

A recent computer model of population oscillation in the hippocampus provides support for our hypothesis that a rhythmic network output can be produced without pacemaker command neurons.[53] The computer model generates a rhythmic activity at a frequency faster than the firing of hippocampal pyramidal cells. As in the thalamus, interneurons fire periodically and are time-locked to the population frequency, even though these cells do not have intrinsic pacemaker properties. However, the hippocampal oscillator model differs from the thalamus in several important aspects. In the computer model, an extensive axon collateral system among pyramidal cells is the basis for the recruitment of additional neurons into population synchrony. Without mutual recurrent excitation, the artificial network is not capable of producing periodic population events. Thalamocortical neurons, however, do not possess widespread local axon collaterals.[23,60] Unlike the computer model of the hippocampus, the immediate cause of cell firing in the thalamus model is the hyperpolarization-triggered low-threshold calcium spike. A further difference is that in the thalamic circuitry, spatial synchrony is explained by the widespread action of GABAergic RT cells and not by excitatory recurrent collaterals. Despite substantially different anatomical organization and ionic conductances of the neuronal elements in the two systems, emergent population oscillation can occur due to the collective co-operation of the elements within the respective networks.

Frequency regulation and N-*methyl*-D-*aspartate receptors*

Another finding of the present experiments was that a blockage of the depolarization-dependent NMDA channels decelerated the clock frequency or even abolished oscillation in the thalamus. Reduction of thalamic network excitability by NMDA blockers decreased the number of participating neurons in HVS (Fig. 9) and increased the intervals between successive population bursts. Interval measurements and power spectral analysis of the HVS indicated that the frequency changes occurred in a stepwise rather than continuous manner. The lowest frequencies observed were slightly below 2 Hz, while the most dominant frequency during NMDA blockade was about 3.5–4 Hz, about half the frequency of the HVS present in the drug-free animal (6–8 Hz). Not infrequently, two or more of the harmonics existed together, either alternating or superimposed on each other (e.g. Fig. 6e) with one dominating over the other(s). It is relevant to reiterate in this context that sleep spindles in the rat have a dominant frequency of 12–16 Hz. These findings suggest that the thalamic clock is capable of producing a much wider range of discrete and overlapping oscillation frequencies than has hitherto been suspected.[19,20,29,47]

In addition to the low-threshold calcium conductance, presumed intradendritic recordings in thalamic cells *in vitro*[19,20] have also revealed a depolarization-dependent, high-threshold Ca^{2+} conductance. This conductance triggers all-or-none depolarizing responses that are followed by the activation of a Ca^{2+}-dependent K^+-mediated afterhyperpolarization. The length of the afterhyperpolarization is very important in the regulation of the refractoriness of the neuron and the timing of re-excitation. Release from hyperpolarization and rebound depolarization of some thalamocortical neurons during the low-threshold calcium spike may be of sufficient magni-

tude and duration to remove the Mg^{2+}-blockade of NMDA channels.[9,50] Opening of the NMDA channels tends to shift the transmembrane potential towards depolarization and therefore may shorten the duration of the afterhyperpolarization. The balance between NMDA-mediated depolarization and the Ca^{2+}- and the voltage-dependent K^+-mediated afterhyperpolarization may determine the re-excitability of individual thalamocortical cells and thereby the frequency of population rhythmicity.

Autoradiographic mapping studies of the thalamus have found a higher density of NMDA-binding in the relay nuclei of the thalamus than in the RT.[4,10,21,34] These findings are compatible with the above suggestion that the possible targets of NMDA channel blockers reside primarily on thalamocortical cells. However, a lower density of NMDA receptors on RT cells does not exclude the possibility that the NMDA blockers act on these neurons as well. Indeed, it is very likely that some volume of the injected ap-5 or ketamine in the present experiments had spread to the RT and exerted their effects on these neurons. The spatial resolution of the present methods is not sufficient to distinguish between these possibilities.

It remains to be clarified if NMDA receptors are involved only in excessive synchrony such as that underlying HVS or if they also play a role in physiological oscillations such as sleep spindles. In support of the involvement of NMDA receptors in the physiological behavior of thalamocortical relay cells, Salt[41,42] reported in the urethane-anesthetized rat that neurons in the ventrobasal thalamus responded to natural tactile stimulation of the vibrissae with prolonged bursts that were attenuated by NMDA antagonists. In sensory transmission, requiring only fast, repetitive single-spike firing, NMDA receptors are probably not involved.[25]

Unilateral infusion of NMDA blockers greatly attenuated the amplitude of HVS and induced slow rhythms, but power peaks at 6–8 Hz have remained in the injected hemisphere. Similarly, unilateral application of NMDA amply increased the amplitude of the spike components without altering the dominant frequency. A possible explanation of these findings is that axons of RT neurons cross the midline to innervate the contralateral relay nuclei.[23] Unilateral damage to the nucleus basalis or RT in previous studies[5] has also failed to produce different HVS frequencies in the two hemispheres. These findings suggest that the two hemispheres of the thalamus work in unison during oscillations.

Neuronal populations involved in high-voltage spindle

The rhythmical output from the thalamus appears to exert a modulatory action on a variety of structures. HVS can be recorded from over virtually the entire neocortex with the spike component dominating over the sensorimotor region.[5] Neocortical neurons, including putative interneurons, fire in association with the spike component of the HVS in rats[5,54] and penicillin-induced spike-and-wave patterns in the cat.[27] Similarly, thalamocortical neurons fire exclusively during the spike component of HVS in various thalamic nuclei, except in the anterior group[5,37] and the lateral habenula.[59] As discussed earlier these nuclei do not receive afferents from the RT[49,55] and their cells do not fire rhythmically during barbiturate spindles in the cat.[35,37] Neurons of the extrapyramidal system can also be recruited into the population synchrony during HVS, including the pallidum, caudate nucleus[5] and pars reticulata of substantia nigra (our unpublished observations). In addition, neurons in the cholinergic nucleus basalis[5] and locus coeruleus (Berridge, Foote and Buzsáki, unpublished observations) also become phase-locked to the HVS. On the other hand, neuronal populations in the hippocampal formation are not affected in any way by the thalamic oscillation.

Although the cause–effect relations among the interactions in these various structures have yet to be worked out, it is clear that very large neuronal populations of spatially distant structures can be entrained during HVS. The phase-locked properties of these cells may assist in the maintenance of long HVS episodes. Conversely, out-of-phase and/or random inputs from various thalamopetal systems are probably important in interfering with rhythmic discharges of thalamic cells and thereby terminating HVS.

Is the neocortex involved in frequency division?

Earlier experiments on penicillin-induced spike-and-wave epilepsy also found frequency shifts from higher frequency barbiturate spindles (8–10 Hz) to lower frequency epileptic spike-and-wave patterns (4–5 Hz) in the cat. The spike-and-wave patterns were thought to result from an elaboration by neocortical circuits on a constant frequency thalamocortical rhythmic input similar to or identical with that producing sleep spindles.[13,15,16,32] It was hypothesized that the penicillin-induced excitability of the cortex is the primary event that produces more efficient recruitment of neocortical neurons in response to an unchanged thalamic input. The increased population synchrony, in turn, results in efficient and long-lasting inhibition of the neocortical pyramidal cells due to increased recurrent inhibition.[13,17] Assuming that the recurrent inhibition lasts longer than the time of arrival of the next thalamic volley, neocortical neurons will fail to respond. These alternating failures will then be the immediate cause of the frequency division of the thalamic clock input and may explain the low frequency of spike-and-wave activity. Several observations of the present experiments argue against this explanation. Firstly, we did not observe a reliable and consistent relationship between large spike components and consecutive failures during HVS episodes (e.g. Fig. 1b). Secondly, the frequency of network bursting in thalamocortical neurons and

RT neurons were identical to the spontaneously occurring HVS. Thirdly, drug-induced frequency shifts of the neocortically recorded HVS and thalamic population bursts were identical. Although the resonance properties of the neocortical circuits, due to enhanced excitability and recurrent inhibition, can significantly enhance thalamic effects, our results suggest that the frequency changes of the rhythmic neocortical events are primarily determined at the level of the thalamus.

Acknowledgements—This work was aided by grants from NIH, the Alzheimer's Disease and Related Disorders Foundation and the Whitehall Foundation. I thank Dr M. Steriade, Dr R. R. Llinás, Dr R. D. Traub and M. Hsu for their comments on the manuscript and Dr F. H. Gage for his support and encouragement.

REFERENCES

1. Andersen P. and Andersson S. A. (1968) *Physiological Basis of the Alpha Rhythm.* Appleton-Century Crofts, New York.
2. Aporti F., Borsato R., Galderini G., Rubini R., Toffano G., Zanotti A., Valzelli L. and Goldstein L. (1986) Age-dependent spontaneous EEG bursts in rats: effect of brain phosphatidylserine. *Neurobiol. Aging* **7,** 115–120.
3. Avoli M., Gloor P., Kostopoulos G. and Gotman J. (1983) An analysis of penicillin-induced generalized spike and wave discharges using simultaneous recordings of cortical and thalamic neurons. *J. Neurophysiol.* **50,** 819–837.
4. Bowery N. G., Wong E. H. F. and Hudson A. L. (1988) Quantitative autoradiography of [^{3}H]-MK-801 binding sites in mammalian brain. *Br. J. Pharmac.* **93,** 944–954.
5. Buzsáki G., Bickford R. G., Ponomareff G., Thal L. J., Mandel R. and Gage F. H. (1988) Nucleus basalis and thalamic control of neocortical activity in the freely moving rat. *J. Neurosci.* **8,** 4007–4026.
6. Buzsáki G., Bickford R. G., Armstrong D. M., Ponomareff G., Chen K. S., Ruiz R., Thal L. J. and Gage F. H. (1988) Electrical activity in the neocortex of freely moving young and aged rats. *Neuroscience* **26,** 735–744.
7. Buzsáki G., Bickford R. G., Ryan L. J., Young S., Prohaska O., Mandel R. S. and Gage F.H. (1989) Multisite recording of brain field potentials and unit activity in freely moving rats. *J. Neurosci. Meth.* **28,** 209–217.
8. Buzsáki G., Smith A., Roskies A. L., Fisher L. J. and Gage F. H. (1989) Parkinsonian tremor and petit mal epilepsy: hypothesis of a common pacemaker. *Neuroscience* **36,** 1–14.
9. Collingridge G. L., Kehl S. J. and McLennan H. (1988) Excitatory amino acids in synaptic transmission in the Schaffer collateral-commissural pathway of the rat hippocampus. *J. Physiol.* **334,** 33–46.
10. Cotman C. W., Monaghan D. T., Ottersen O. P. and Storm-Mathisen J. (1987) Anatomical organization of excitatory amino acid receptors and their pathways. *Trends Neurosci.* **10,** 273–280.
11. Deschenes M., Madariaga-Domich A. and Steriade M. (1985) Dendrodendritic synapses in the cat reticularis thalami nucleus: a structural basis for thalamic spindle synchronization. *Brain Res.* **334,** 165–168.
12. Domich L., Oakson G. and Steriade M. (1986) Thalamic burst patterns in the naturally sleeping cat: a comparison between cortically projecting and reticularis neurons. *J. Physiol., Lond.* **379,** 429–449.
13. Giaretta D., Avoli M. and Gloor P. (1987) Intracellular recordings in pericruciate neurons during spike and wave discharges of feline generalized penicillin epilepsy. *Brain Res.* **405,** 68–79.
14. Gloor P. (1979) Generalized epilepsy with spike-and-wave discharge: a reinterpretation of its electrographic and clinical manifestations. *Epilepsia* **20,** 571–588.
15. Gloor P. (1984) Electrophysiology of generalized epilepsy. In *Electrophysiology of Epilepsy* (eds Schwartzkroin P. A. and Wheal H.), pp. 107–136. Academic Press, London.
16. Gloor P., Pellegrini A. and Kostopoulos G. K. (1979) Effects of changes in cortical excitability upon the epileptic bursts in generalized penicillin epilepsy of the cat. *Electroenceph. clin. Neurophysiol.* **46,** 274–289.
17. Gloor P. and Fariello R. G. (1988) Generalized epilepsy: some of its cellular mechanisms differ from those of focal epilepsy. *Trends Neurosci.* **11,** 63–68.
18. Houser C. R., Vaughn J. E., Barber R. P. and Roberts E. (1980) GABA neurons are the major cell type of the nucleus reticularis thalami. *Brain Res.* **200,** 431–435.
19. Jahnsen H. and Llinás R. R. (1984) Electrophysiological properties of guinea pig thalamic neurones: an *in vitro* study. *J. Physiol.* **249,** 205–226.
20. Jahnsen H. and Llinás R. R. (1984) Ionic basis for the electroresponsiveness and oscillatory properties of guinea-pig thalamic neurons *in vitro*. *J. Physiol.* **349,** 227–247.
21. Jarvis M. F., Murphy D. E. and Williams M. (1987) Quantitative autoradiographic localization of NMDA receptors in rat brain using [^{3}H]CPP: comparison with [^{3}H]TCP binding sites. *Eur. J. Pharmac.* **141,** 149–152.
22. Jasper H. H. and Droogleever-Fortuyn J. (1946) Experimental studies on the functional anatomy of petit mal epilepsy. *Res. Publs Ass. Res. nerv. ment. Dis.* **26,** 272–298.
23. Jones E. G. (1985) *The Thalamus.* Plenum, New York.
24. King G. A. and Burnham W. M. (1982) Alpha-2 adrenergic antagonists suppress epileptiform EEG activity in a petit mal seizure model. *Life Sci.* **30,** 293–298.
25. Klockgether T. (1987) Excitatory amino acid receptor-mediated transmission of somatosensory evoked potentials in the rat thalamus. *J. Physiol., Lond.* **394,** 445–461.
26. Kostopoulos B., Gloor P., Pellegrini A. and Siatsas I. (1981) A study of the transition from spindles to spike and wave discharge in feline generalized penicillin epilepsy: EEG features. *Expl Neurol.* **73,** 43–54.
27. Kostopoulos B., Gloor P., Pellegrini A. and Gotman J. (1981) A study of the transition from spindles to spike and wave discharge in feline generalized penicillin epilepsy: microphysiological features. *Expl Neurol.* **73,** 55–77.
28. Kristiansen K. and Courtois G. (1949) Rhythmic electrical activity from isolated cerebral cortex. *Electroenceph. clin. Neurophysiol.* **1,** 265–272.
29. Llinás R. R. (1988) The intrinsic electrophysiological properties of mammalian neurons: insight into central nervous system function. *Science* **242,** 1654–1664.
30. Llinás R. R. and Geijo-Barrientos E. (1988) *In vitro* studies of mammalian thalamic and reticularis neurons. In *Cellular Thalamic Mechanisms* (eds Bentivoglio M. and Spreafico R.), pp. 23–33. Elsevier, Amsterdam.
31. McCormick D. A. and Prince D. A. (1986) Acetylcholine induces burst firing in thalamic reticular neurons by activating a potassium conductance. *Nature* **319,** 402–405.

32. McLachlan R. S., Avoli M. and Gloor P. (1984) Transition from spindles to generalized spike and wave discharges in the cat: simultaneous single-cell recordings in cortex and thalamus. *Expl Neurol.* **85,** 413–425.
33. Micheletti G., Warter J.-M., Marescaux C., Depaulis A., Tranchant C., Rumbach L. and Vergnes M. (1987) Effects of drugs affecting noradrenergic neurotransmission in rats with spontaneous petit mal-like seizures. *Eur. J. Pharmac.* **135,** 397–402.
34. Monaghan D. T. and Cotman C. W. (1985) Distribution of *N*-methyl-D-aspartate-sensitive L[^{3}H]glutamate binding sites in rat brain. *J. Neurosci.* **5,** 2909–2919.
35. Mulle C., Steriade M. and Deschenes M. (1985) Absence of spindle oscillations in the cat anterior thalamic nuclei. *Brain. Res.* **334,** 169–171.
36. Ohara P. T. and A. R. Lieberman (1985) The thalamic reticular nucleus of the adult rat: experimental anatomical studies. *J. Neurocytol.* **14,** 365–411.
37. Pare D., Steriade M., Deschenses M. and Oakson G. (1987) Physiological properties of anterior thalamic nuclei, a group devoid of inputs from the reticular thalamic nucleus. *J. Neurophysiol.* **57,** 1669–1685.
38. Prince D. and Farell D. (1969) "Centrencephalic" spike-wave discharges following parenteral penicillin injection in the cat. *Neurology* **19,** 309–310.
39. Racine R. J. (1972) Modification of seizure activity by electrical stimulation: II. Motor seizure. *Electroenceph. clin. Neurophysiol.* **32,** 211–294.
40. Roy J. P., Clercq M., Steriade M. and Deschenes M. (1984) Electrophysiology of neurons of lateral thalamic nuclei in cat: mechanisms of long-lasting hyperpolarizations. *J. Neurophysiol.* **51,** 1220–1235.
41. Salt T. E. (1986) Mediation of thalamic sensory input by both NMDA receptors and non-NMDA receptors. *Nature* **322,** 263–265.
42. Salt T. E. (1987) Excitatory amino acid receptors and synaptic transmission in the rat ventrobasal nucleus. *J. Physiol.* **391,** 499–510.
43. Shosaku A., Kayama Y., Sumimoto I., Sugitani M. and Iwama K. (1989) Analysis of recurrent inhibitory circuit in rat thalamus: neurophysiology of the thalamic reticular nucleus. *Prog. Neurobiol.* **32,** 77–102.
44. Spreafico R., DeCurtis M., Frassoni C. and Avanzini G. (1988) Electrophysiological characteristics of morphologically identified reticular thalamic neurons from rat slices. *Neuroscience* **27,** 629–638.
45. Steriade M. (1991) Spindling, incremental thalamocortical responses, and spike and wave epilepsy. In *Generalized Epilepsy* (eds Avoli M., Gloor P., Kostopoulos G. and Naquet R.). Birkhauser, Boston (in press).
46. Steriade M. and Deschenes M. (1988) In *Cellular Thalamic Mechanisms* (eds Bentivoglio M. and Spreafico R.), pp. 37–62. Elsevier, Amsterdam.
47. Steriade M. and Llinás R. R. (1988) The functional states of the thalamus and the associated neuronal interplay. *Physiol. Rev.* **68,** 649–741.
48. Steriade M. and Buzsáki G. (1990) Parallel activation of the thalamus and neocortex. In *Brain Cholinergic Systems* (eds Steriade M. and Biesold D.). Oxford University Press, Oxford.
49. Steriade M., Parent A. and Hada J. (1984) Thalamic projections of nucleus reticularis thalami of cat: a study using retrograde transport of horseradish peroxidase and fluorescent tracers. *J. comp. Neurol.* **229,** 531–547.
50. Steriade M., Deschenes M., Domich L. and Mulle C. (1985) Abolition of spindle oscillation in thalamic neurons disconnected from nucleus reticularis thalami. *J. Neurophysiol.* **54,** 1473–1497.
51. Steriade M., Domich L. and Oakson G. (1986) Reticularis thalami neurons revisited: activity changes during shifts in states of vigilance. *J. Neurosci.* **6,** 68–81.
52. Steriade M., Domich L., Oakson G. and Deschenes M. (1987) The deafferented reticular thalamic nucleus generates spindle rhythmicity. *J. Neurophysiol.* **57,** 260–273.
53. Traub R. D., Miles R. and Wong R. K. S. (1989) Model of rhythmic population oscillation in the hippocampal slice. *Science* **243,** 1319–1325.
54. Vanderwolf C. H. (1988) Cerebral activity and behavior: control by central cholinergic and serotonergic system. *Int. Rev. Neurobiol.* **30,** 225–340.
55. Velayos J. L., Jimenez-Castellanos J. Jr and Reinoso-Suares F. (1989) Topographical organization of the projections from the reticular thalamic nucleus to the intralaminar and medial thalamic nuclei. *J. comp. Neurol.* **279,** 457–469.
56. Vergnes M., Marescau C., Depaulis A., Micheletti G. and Warter J. M. (1986) Ontogeny of spontaneous petit mal-like seizures in Wistar rats. *Devl Brain Res.* **30,** 85–87.
57. Vergnes M., Marecaux C., Depaulis A., Micheletti G. and Warter J. M. (1987) Spontaneous spike and wave discharges in thalamus and cortex in a rat model of genetic petit mal-like seizure. *Expl Neurol.* **96,** 127–136.
58. Watkins J. C. and Olverman H. J. (1987) Agonists and antagonists for excitatory amino acid receptors. *Trends Neurosci.* **10,** 265–272.
59. Wilcox K. S., Gutnick M. J. and Christoph G. R. (1989) Electrophysiological properties of neurons in the lateral habenula nucleus: an *in vitro* study. *J. Neurophysiol.* **59,** 212–225.
60. Yen C. T. and Jones E. G. (1985) Intracellular staining of physiologically identified neurons and axons in the somatosensory thalamus of the cat. *Brain Res.* **280,** 148–154.
61. Yen C. T., Conley M., Hendry S. H. C. and Jones E. G. (1985) The morphology of physiologically identified GABAergic neurons in the somatic sensory part of the thalamic reticular nucleus in the cat. *J. Neurosci.* **5,** 2254–2268.

(*Accepted* 19 *September* 1990)